Journal of Southeast University (English Edition) Vol. 27, No. 3, pp. 300 – 304 Sept. 2011 ISSN 1003—7985

Acoustic emission source identification based on harmonic wavelet packet and support vector machine

Yu Jintao[1,2] Ding Mingli[1] Meng Fangang[3] Qiao Yuliang[3] Wang Qi[1]

([1] Department of Automatic Measurement and Control, Harbin Institute of Technology, Harbin 150001, China)
([2] School of Computer and Information Engineering, Harbin University of Commerce, Harbin 150028, China)
([3] Harbin Aviation Industry Group Co. Ltd., Harbin 150066, China)

Abstract: In order to solve the fatigue damage identification problem of helicopter moving components, a new approach for acoustic emission (AE) source type identification based on the harmonic wavelet packet (HWPT) feature extraction and the hierarchy support vector machine (H-SVM) classifier is proposed. After a four-level decomposition of the HWPT, the energy feature of AE signals in different frequency bands is extracted, which overcomes the shortcomings of the traditional wavelet packet including energy leakage, and inflexible frequency band selection and different frequency resolutions on different levels. The H-SVM classifier is trained with a subset of the experimental data for known AE source types and tested using the remaining set of data. The results of pressure-off experiments on the specimens of carbon fiber materials indicate that the proposed approach can effectively implement the AE source type identification, and has a better performance in terms of computational efficiency and identification accuracy than the wavelet packet (WPT) feature extraction.

Key words: harmonic wavelet packet; hierarchy support vector machine; acoustic emission source identification
doi: 10.3969/j.issn.1003 – 7985.2011.03.015

Due to the fact that helicopter moving components easily produce fatigue damage such as cracks, which can seriously endanger the operating stability and the safety of helicopters. It is necessary to monitor the initiation of cracks and to master the developing trend of the cracks.

Acoustic emission (AE) is a noticeable choice of the non-destructive testing methods due to its extremely high sensitivity. AE has proved to be a very sensitive method for defect recognition of composite materials which has been used in typical application areas such as aerospace, vehicle industry and infrastructure. The automatic recognition of defect types based on AE signals has attracted much attention and recently many studies have been published [1-2]. In the AE technique, the AE source type identification is used to determine the type of fatigue damage.

The AE source type identification is a typical pattern recognition problem, which includes two steps: feature extraction and pattern classification. AE signals are non-stationary signals, so the traditional techniques in the time and frequency domains are not suitable. The wavelet transform (WT) is demonstrated as an alternative tool for feature extraction. The scaling operation in wavelet transform produces a series of wavelet functions with different window sizes, enabling multi-resolution analysis suitable for representing non-stationary signals. A major drawback of the wavelet transform is its low-frequency resolution in the high frequency region. The wavelet packet transform (WPT), in comparison, further decomposes the detailed information of the signal, which has been successfully applied in the feature extraction of sensor fault and machine health diagnosis[3-4]. Of the various types of wavelets developed, the harmonic wavelet possesses compact frequency expression and has overcome shortcomings such as energy leakage, inflexible frequency band selection and different frequency resolutions on different levels of the traditional wavelet[5]. So in this paper, the harmonic wavelet packet transform is used to extract the features of AE sources.

Numerous pattern recognition methods are developed based on intelligent systems. Among them, the statistical learning method and the artificial neural network (ANN) are mostly used in AE signals analyses of composite materials. The ANN is widely applied in AE signal classification problems based on learning patterns from samples or empirical data modeled in the last two decades [6-7]. However, as a typical machine learning classifier, the ANN method is based on the empirical risk minimization principle, which has been recognized as a method that cannot always minimize the actual risks. Meanwhile, the effectiveness of the ANN methods is closely related to the number of training samples. In most cases, it is difficult to obtain large sample sets of AE signals in composite materials and the effectiveness of the ANN methods can hardly be improved. In order to overcome the disadvantages of the ANN, the support vector machine (SVM) is used for the classification of AE sources. The SVM based on the statistical learning theory has high accuracy and good generalization capability. It is very suitable for pattern recognition with small samples.

In this paper, we discuss the application of the harmonic wavelet packet feature extraction and the support vector machine classification in AE source type identification, and verify the algorithm using pressure-off experiments on the specimens of carbon fiber materials.

1 Feature Extraction Based on Harmonic Wavelet Packet

1.1 Harmonic wavelet

In essence, the wavelet transform characterizes the correlation or similarity between the signal to be analyzed and the

Received 2011-05-06.
Biographies: Yu Jintao (1974—), male, graduate; Wang Qi (corresponding author), male, master, professor, wangqi@hit.edu.cn.
Foundation items: The Natural Science Foundation of Heilongjiang Province (No. F201018), the National Natural Science Foundation of China (No. 60901042).
Citation: Yu Jintao, Ding Mingli, Meng Fangang, et al. Acoustic emission source identification based on harmonic wavelet packet and support vector machine [J]. Journal of Southeast University (English Edition), 2011, 27(3): 300 – 304. [doi: 10.3969/j.issn.1003 – 7985.2011.03.015]

mother wavelet function. Such a correlation is expressed by the wavelet coefficients associated with the wavelet transform, which can be calculated through a correlation operation between the signal $x(t)$ and the conjugate $\overline{w}(t)$ of the chosen mother wavelet $w(t)$:

$$W(t) = \int_{-\infty}^{+\infty} x(\tau)\,\overline{w}(\tau - t)\,\mathrm{d}\tau \tag{1}$$

If the signal $x(t)$ is closely correlated with the mother wavelet $w(t)$, the value of the wavelet coefficient $\overline{w}(t)$ will be high, indicating a good match between the mother wavelet and the signal being analyzed. As a result, information embedded in the signal can be extracted by analyzing the wavelet coefficients with local maxima. In 1993, Professor Newland [8-10] from Cambridge University proposed the harmonic wavelet which has ideal box-like characteristics in the frequency domain. In this study, the harmonic wavelet is chosen as the mother wavelet due to the simplicity of its expression in the frequency domain, which is defined as

$$H_{m,n}(\omega) = \begin{cases} \dfrac{1}{2\pi(n-m)} & m2\pi \leqslant \omega \leqslant n2\pi \\ 0 & \text{otherwise} \end{cases} \tag{2}$$

where m and n are the scale parameters. These parameters are real but not necessarily integers. By taking the inverse Fourier transform of $H_{m,n}(\omega)$, the time domain expression of the harmonic wavelet is obtained,

$$h_{m,n}(t) = \frac{\mathrm{e}^{(in2\pi t)} - \mathrm{e}^{(im2\pi t)}}{i2\pi(n-m)t} \tag{3}$$

If the harmonic wavelet is translated by a step $k/(n-m)$ and $k \in \mathbf{Z}$, in which k is the translation parameter, a generalized expression that is centered at $t = k/(n-m)$ with a bandwidth of $2(n-m)\pi$ can be written as

$$h_{m,n}\left(t - \frac{k}{n-m}\right) = \frac{\exp\left[in2\pi\left(t - \dfrac{k}{n-m}\right)\right] - \exp\left[im2\pi\left(t - \dfrac{k}{n-m}\right)\right]}{i2\pi(n-m)\left(t - \dfrac{k}{n-m}\right)} \tag{4}$$

Based on the generalized expression, the harmonic wavelet transform of a signal $x(t)$ can be performed as

$$\mathrm{hwt}(m, n, k) = \frac{n-m}{N}\sum_{r=0}^{N-1} x(r)\,h_{m,n}\left(r - \frac{k}{n-m}\right) \tag{5}$$

where $\mathrm{hwt}(m, n, k)$ is the harmonic wavelet coefficient. By the Fourier transform of Eq. (5), an equivalent expression of the harmonic wavelet transform in the frequency domain can be expressed as

$$\mathrm{HWT}(m, n, \omega) = X(\omega)\,\overline{H}_{m,n}[(n-m)\omega] \tag{6}$$

where $X(\omega)$ is the Fourier transform of the signal $x(t)$, and $\overline{H}_{m,n}[(n-m)\omega]$ is the conjugate of $H_{m,n}[(n-m)\omega]$, which is the Fourier transform of the harmonic wavelet at the scale (m, n). Since the harmonic wavelet has compact frequency expression, as shown in Eq. (2), the harmonic wavelet transform can be readily obtained through a pair of the Fourier transform and inverse Fourier transform operations.

As shown in Fig. 1, after taking the Fourier transform of a signal $x(t)$ to obtain its frequency domain expression $X(\omega)$, the inner product $\mathrm{HWT}(m, n, \omega)$ of $X(\omega)$ and the conjugate of the harmonic wavelet $\overline{H}_{m,n}[(n-m)\omega]$ at the scale (m, n) are calculated. Finally, the harmonic wavelet transform of the signal $x(t)$, denoted as $\mathrm{hwt}(m, n, k)$, is obtained by taking the inverse Fourier transform of the inner product $\mathrm{HWT}(m, n, \omega)$.

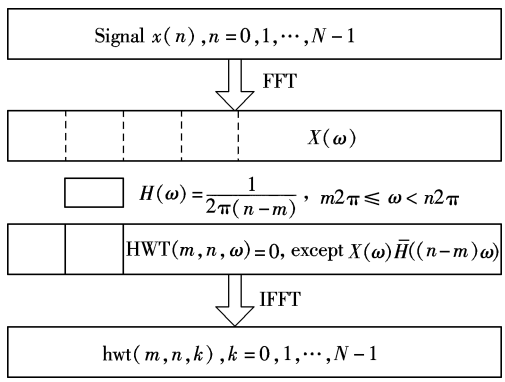

Fig. 1 Algorithm for implementing harmonic wavelet transform

1.2 Harmonic wavelet packet algorithm

The scale parameter m and n determine the bandwidth that the harmonic wavelet covers. Similar to the wavelet packet transform (WPT), the number of frequency sub-bands for the harmonic wavelet packet transform (HWPT) has to be s powers of two, in which s corresponds to the decomposition level for the WPT. Accordingly, the signal can be decomposed into 2^s frequency sub-bands, with the bandwidth in Hz for each sub-band defined by

$$f_{\mathrm{band}} = \frac{f_{\mathrm{h}}}{2^s} \tag{7}$$

where f_{h} is the highest frequency component of the signal to be analyzed. Since the bandwidth of the harmonic wavelet is $2(n-m)\pi$, the selection of the values for m and n of the HWPT must satisfy the following conditions:

$$2(n-m)\pi = 2\pi f_{\mathrm{band}} \tag{8}$$

Thus, the harmonic wavelet packet coefficients $\mathrm{hwpt}(s, i, k)$ can be obtained as

$$\mathrm{hwpt}(s, i, k) = \mathrm{hwt}(m, n, k) \tag{9}$$

where i is the index of the sub-band, and k is the index of the coefficient. The parameters m and n are required to satisfy the following condition:

$$m = if_{\mathrm{band}} = i\frac{f_{\mathrm{h}}}{2^s},\quad n = (i+1)f_{\mathrm{band}} = (i+1)\frac{f_{\mathrm{h}}}{2^s} \tag{10}$$

where $i = 0, 1, \ldots, 2^s - 1$.

1.3 AE signal feature extraction

With the AE signal being decomposed into a number of

sub-bands, features can be extracted from the harmonic wavelet packet coefficients in each sub-band to provide information on the type of AE sources. Different energy distributions of signals at different frequency bands must be caused by different information contained in the signals. For the AE signal, it is because of different AE source features. Therefore, the characteristic energy distribution coefficients of the harmonic wavelet packet are used as the feature vectors. The energy content of a signal can be calculated based on the coefficients of the signal transform. In the case of a HWPT, the coefficients $hwpt(s, i, k)$ quantify the energy associated with each specific sub-band. The detail of the feature extraction procedure is shown as follows:

Step 1 Normalize the AE signal by

$$\widetilde{\boldsymbol{X}} = D_{\sigma}^{-1}[\boldsymbol{X} - E(\boldsymbol{X})] \tag{11}$$

where $\boldsymbol{X}$ is the AE signal, $E(\boldsymbol{X})$ and D_{σ} are the mean and standard deviation of $\boldsymbol{X}$.

Step 2 Decompose $\widetilde{\boldsymbol{X}}$ with four levels of harmonic wavelet packet transforms and obtain the coefficient vectors of sixteen nodes, $H_{4,0}, H_{4,1}, \ldots, H_{4,15}$, where $H_{4,i}$ represents hwpt$(4, i, k)$, $k = 0, 1, \ldots, N-1$, and N is the length of the AE signal.

Step 3 Calculate the energy of each node and normalize them.

$$E_{H_{4,i}} = \int |H_{4,i}|^2 \mathrm{d}t = \sum_{j=1}^{N} |H_{4,i,j}|^2 \tag{12}$$

$$\overline{E}_{H_{4,i}} = \frac{E_{H_{4,i}}}{\sqrt{\sum_{i=0}^{15} |E_{H_{4,i}}|^2}} \tag{13}$$

Step 4 The feature vector $\boldsymbol{T} = [\overline{E}_{H_{4,0}}, \overline{E}_{H_{4,1}}, \overline{E}_{H_{4,2}}, \cdots, \overline{E}_{H_{4,15}}]$ is used to identify the AE source types.

2 AE Source Identification Using Hierarchy SVM Classifier

AE source identification is a typical pattern recognition problem with small samples, because in most cases, it is difficult to obtain large sample sets of AE signals in composite materials to train the classifiers. In this paper, the SVM is selected as the basic classifier, because it provides a novel approach to the two-category classification problem with good small sample generation [11-12].

There are two standard approaches to construct and combine the results from binary classifiers for a C-class problem. The first is the one-versus-rest method, in which each classifier distinguishes one class from the other $C-1$ classes, and the class label of the input is determined by the winner-take-all method[13]. Each classifier needs to be trained on the whole training set, and there is no guarantee that good discrimination exists between one class and the remaining classes. The second standard approach to combine binary classifiers is the one-versus-one method, in which the decision is made by majority voting strategies. This requires training and testing of $C(C-1)/2$ binary classifiers. This approach is prohibitive when C is large [14].

We choose a binary hierarchical classification structure as shown in Fig. 2. Each node is a binary classifier, coarse separation between classes occurs at the beginning (at upper levels) in the hierarchy and a finer classification decision later (at lower levels). At the top node, we divide the original four classes into two smaller groups of classes (macro-classes). This clustering procedure is repeated at subsequent levels, until there is only one class in the final sub-group. This hierarchical structure decomposes the problem into three binary sub-problems. For testing, only about $\log_2 3$ classifiers are required to traverse a path from top to bottom.

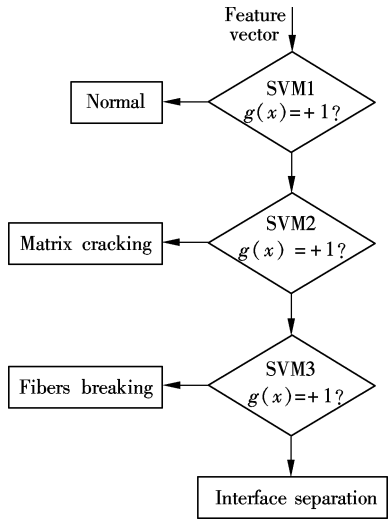

Fig. 2 Hierarchical multi-classification structure for AE source identification

In this paper, standard k-means clustering is used to design the binary hierarchical structure, and Fig. 2 shows the result. SVM1 is used to classify normal versus other three patterns, SVM2 is used to classify matrix cracking versus fibers breaking, and SVM3 is used to classify fibers breaking versus interface separation.

In the training phase, the training samples are grouped according to Fig. 2. Then SVM1 to SVM3 are trained using the corresponding group of training samples. After that, by inputting the feature vector into the trained multi-classifier, the AE source type can be identified.

3 Experiment and Results

3.1 Experimental setup

In order to verify the proposed method, a series of pressure off experiments are carried out on the specimens of carbon fiber materials, which is one of the commonly used materials of helicopter moving components. Fig. 3 shows the pressure-off experiment process on a carbon fiber specimen. The dimensions of all the samples are 418 mm × 120 mm × 2 mm. Two AE sensors are distributed on the carbon fiber specimen, one is an 80-mm distance away from the central line of the specimen in the up direction, the other is an 80-mm distance away from the central line of the specimen in the down direction. The central point of the specimen is the force point. The loading speed of the pressure off experiment is 500 N/s. The AE signal measurement system is shown schematically in Fig. 4. Signal conditioning is performed by pre-amplifiers. The conditioning signal (with a gain of 40 dB) is fed to the main data-acquisition board, in

which the AE waveforms and parameters are stored. The instrument and equipments used in the experiments are listed below: MTS electro-hydraulic loading system (MTS 810 material test system); Vallen AMSY-5 AE signal acquisition system with 16 channels and a 16-bit, 10-MHz AD converter on each channel; Vallen VS150-M AE sensor; Vallen AEP4 pre-amplifier (20-2000 kHz); Vallen AE application software Vallen Visual AE.

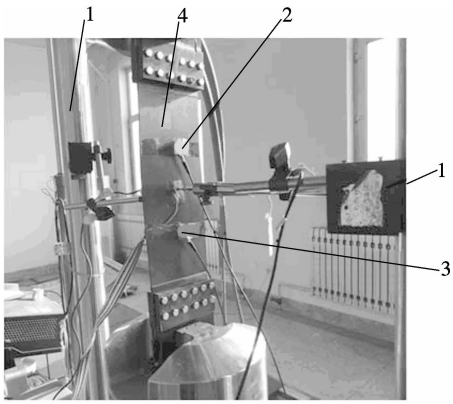

1—MTS electro-hydraulic loading system; 2—AE sensor 1
3—AE sensor 2; 4—Carbon fiber specimen

Fig. 3 Pressure off experiment process on carbon fiber specimen

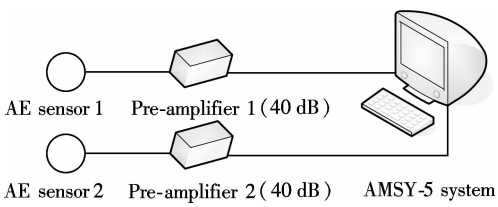

Fig. 4 AE acquisition system employed on-site

The sample rate of the acquisition system is 1 MHz. In order to acquire all the AE signals during the pressure off process, AMSY-5 works under the continuous acquisition mode. The pressure-off experiments are conducted on three specimens of carbon fiber materials with the same dimensions. For each AE source type, 50 groups of data are gathered.

3.2 Feature extraction

First, the experiment of feature extraction is performed according to the algorithm given in section 1.3. Tab. 1 shows the feature nodes and their frequency ranges. The frequency band for each feature node is 31.25 kHz. Fig. 5 shows the normalized energy distribution for different AE sources at 15 frequency sub-bands.

As shown in Fig. 5, the energy distribution of the normal state is approximately uniform in each frequency band, because the AE signal of the normal state is approximately white noise. The energy distribution of matrix cracking is mainly concentrated in frequency bands 3, 4 and 5. The energy distribution of fibers breaking is mainly concentrated in frequency bands 4, 5, 6, and 7. The energy distribution of interface separation is broad, approximately from frequency bands 3 to 8. Therefore, combining the above analyses, the AE source types can be distinguished using the harmonic wavelet packet energy features.

Tab. 1 Feature nodes and their frequency band range

Feature nodes	Frequency band number	Frequency band range/kHz
$H_{4,0}$	0	0 to 31.25
$H_{4,1}$	1	31.25 to 62.50
$H_{4,2}$	2	62.50 to 93.75
⋮	⋮	⋮
$H_{4,13}$	13	40.625 to 43.75
$H_{4,14}$	14	43.75 to 468.75
$H_{4,15}$	15	468.75 to 500.00

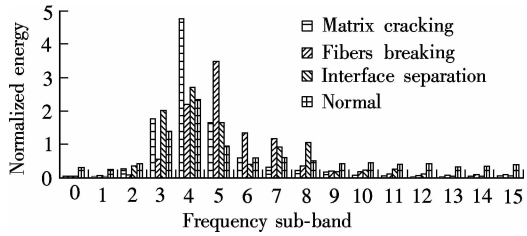

Fig. 5 Normalized energy distribution for different AE sources at 15 frequency sub-bands

3.3 AE source identification using H-SVM classifier

After the experiment of feature extraction, two groups of data, the training samples and the testing data are acquired. 20 groups of data for each type are used as training samples, and 30 groups of data for each type are used as testing data. The H-SVM classifier is trained using the training samples according to section 2. The kernel functions of the three SVMs in the H-SVM classifier are selected as RBF kernels,

$$K(\boldsymbol{X}_i, \boldsymbol{X}_j) = \exp(-\|\boldsymbol{X}_i - \boldsymbol{X}_j\|^2/\sigma^2) \qquad (14)$$

The kernel width parameter, σ for each SVM, is selected as 1.0. Tab. 2 shows the AE source identification result using HWPT and H-SVM. The results indicate that the proposed approach can implement AE source type identification effectively.

Tab. 2 AE source identification result using HWPT and H-SVM

AE source type	Test sample number (correct number)	Identification rate/%
Matrix cracking	30(28)	93.33
Fibers breaking	30(27)	90.00
Interface separation	30(28)	93.33
Normal	30(30)	100.00

In order to verify the advantages of HWPT feature extraction, the comparison of WPT feature extraction and H-SVM classifier with HWPT and H-SVM is studied. For the WPT feature extraction, the wavelet function is select as Db10, and the decomposing level is 4. Similar to the HWPT feature extraction, the feature vector of the WPT is also the normalized energy in each frequency band. Tab. 3 shows the comparison of feature extraction time for the HWPT and the WPT. These algorithms are all implemented by Matlab 7.1 on Intel Dual Core 2.4 GHz and 1 GB RAM. The results indicate that the feature extraction speed of the HWPT is over nine times as quick as the WPT. Such an advantage of the HWPT over the WPT is even more appreciable when the decomposition level is greater than 4, because of the additional recursive operations needed for the WPT.

Tab. 3 Feature extraction time comparison of HWPT and WPT

Feature extraction method	Feature extraction time for 50 sample/s
HWPT	0.65
WPT	5.88

Tab. 4 shows the comparison of AE source identification result for HWPT and H-SVM with WPT and H-SVM. The results indicate that the identification rate of HWPT and H-SVM is a little higher than for that of WPT and H-SVM. HWPT overcomes the energy leakage shortcoming of the traditional wavelet and can extract the energy features more accurately.

Tab. 4 AE source identification comparison of HWPT and H-SVM with WPT and H-SVM

AE source type	Identification rate/%	
	HWPT and H-SVM	WPT and H-SVM
Matrix cracking	93.33	86.67
Fibers breaking	90.00	83.33
Interface separation	93.33	90.00
Normal	100.00	100.00

4 Conclusion

In this paper, the HWPT feature extraction and the H-SVM classifier is first applied to the AE source identification. The experimental system is set up and the pressure-off experiments on the specimens of carbon fiber materials are carried out. The comparison of the HWPT and the H-SVM with the WPT and the H-SVM indicates that the proposed approach can effectively implement AE source type identification and has better performance in computational efficiency and identification accuracy than that of WPT feature extraction. The efficient energy feature extraction ability and better computational efficiency makes the HWPT a good candidate for efficient on-line AE source identification.

References

[1] Tittmann B R, Yen C E. Acoustic emission technique for monitoring the pyrolysis of composites for process control [J]. *Ultrasonics*, 2008, **48**(6/7): 621 - 630.

[2] Liu Q, Chen X. Fuzzy pattern recognition of AE signals for grinding burn [J]. *Machine Tools & Manufacture*, 2005, **45**(7/8): 811 - 818.

[3] Zhou Rui, Bao Wen, Li Ning, et al. Mechanical equipment fault diagnosis based on redundant second generation wavelet packet transform [J]. *Digital Signal Processing*, 2010, **20**(1): 276 - 288.

[4] Feng Zhigang, Wang Qi, Shida K. Design and implementation of a self-validating pressure sensor [J]. *IEEE Sensors Journal*, 2009, **9**(3): 207 - 218.

[5] Zhang Wenbin, Zhou Xiaojun, Lin Yong, et al. Harmonic wavelet package method used to extract fault signal of a rotation machinery [J]. *Journal of Vibration and Shock*, 2009, **28**(3): 87 - 89. (in Chinese)

[6] Zhao Yuanxi, Xu Yonggang, Gao Lixin, et al. Fault pattern recognition technique for roller bearing acoustic emission based on harmonic wavelet packet and BP neural network [J]. *Journal of Vibration and Shock*, 2010, **29**(10): 162 - 165;257. (in Chinese)

[7] Emamian V, Kaveh M, Tewfik A H, et al. Robust clustering of acoustic emission signals using neural networks and signal subspace projections [J]. *EURASIP Journal on Applied Signal Processing*, 2003, **2003**(3): 276 - 286.

[8] Newland D E. Harmonic wavelet analysis [J]. *Proceedings of the Royal Society A*, 1993, **443**(1917): 203 - 225.

[9] Newland D E. Wavelet analysis of vibration, part 1: theory [J]. *Journal of Vibration and Acoustic*, 1994, **116**(4): 409 - 416.

[10] Newland D E. Wavelet analysis of vibration, part 2: wavelet map [J]. *Journal of Vibration and Acoustic*, 1994, **116**(4): 417 - 425.

[11] Qian Huimin, Mao Yaobin, Xiang Wenbo, et al. Recognition of human activities using SVM multi-class classifier [J]. *Pattern Recognition Letters*, 2010, **31**(2): 100 - 111.

[12] Avci D, Varol A. An expert diagnosis system for classification of human parasite eggs based on multi-class SVM [J]. *Expert Systems with Applications*, 2009, **36**(1): 43 - 48.

[13] Anand J R, Mehrotra K, Mohan C K, et al. Efficient classification for multiclass problems using modular neural networks [J]. *IEEE Transactions on Neural Networks*, 1995, **6**(1): 117 - 124.

[14] Kumar S, Ghosh J, Crawford M M. Hierarchical fusion of multiple classifiers for hyper spectral data analysis [J]. *Pattern Analysis and Applications*, 2002, **5**(2): 210 - 220.

基于谐波小波包和支持向量机的声发射源识别

于金涛[1,2] 丁明理[1] 孟凡刚[3] 乔玉良[3] 王 祁[1]

([1] 哈尔滨工业大学自动化测试与控制系,哈尔滨 150001)
([2] 哈尔滨商业大学计算机与信息工程学院, 哈尔滨 150028)
([3] 哈尔滨航空工业集团, 哈尔滨 150066)

摘要:为了解决直升机动部件疲劳损伤类型识别问题,提出了一种基于谐波小波包特征提取和层次支持向量多分类器的声发射源类型识别方法. 声发射信号经过4层谐波小波包分解后,提取各个频段的能量特征用于声发射源类型识别,克服了传统小波包分析能量泄露、频带选取不灵活、不同层频率分辨率不同的缺点. 首先,利用已知声发射源类型的试验数据训练层次支持向量多分类器,然后,利用其余试验数据进行测试. 碳纤维材料试件压断试验结果表明:该方法有效地实现了声发射源多类识别,并且在计算效率和识别精度上都优于小波包特征提取方法.

关键词:谐波小波包;层次支持向量机;声发射源识别
中图分类号:TG115.28